

Optimal electronic transitions in a simple two-band model

A. Dargys*

Semiconductor Physics Institute, A. Goštauto 11, 2600 Vilnius, Lithuania

(Received 24 May 2001; revised manuscript received 31 July 2001; published 28 November 2001)

A quantum-mechanical problem of coherent control of charge-carrier transfer dynamics between two parabolic and spherical energy bands using optical electric fields was solved within the effective-mass approximation. Starting from the Luttinger-Kohn Hamiltonian, the problem at first was reduced to a single time-dependent Schrödinger-like equation for coherent hole transitions between two bands. Then, the obtained equation and the functional that minimizes the energy of optical pulse are used to deduce the Euler equation for optimal control. The multiplicity of the quantum-control problem is demonstrated explicitly. An example of interband excitation with an optimal π -type monopulse is presented.

DOI: 10.1103/PhysRevB.64.235123

PACS number(s): 78.47.+p, 42.65.Pc, 42.65.Sf

I. INTRODUCTION

By tailoring the shape of electromagnetic pulse it is possible to manipulate constructive and destructive interference of a quantum system and in this way to achieve the desired final state of the system at the end of the perturbation. In the case of quantum control in solids, the duration of the optical pulse must be shorter than or, at least, comparable to the shortest scattering time by lattice phonons to preserve the coherence of the quantum transition. The optimization of optical pulses, in general, is a complex multidimensional control problem.¹⁻¹⁷ In quantum mechanics the control is not unique,¹³ and should be treated as a quantum-mechanical rather than a classical measurement process. In Ref. 13 it has been argued that there will be “denumerably infinite number of solutions” to a well-posed quantum-mechanical optimal control problem. It is important to stress that the control and observation of the quantum systems takes place in a real space rather than in an abstract Hilbert space of state vectors. Thus, quantum-control methods that consider the guidance of a state vector from one point to the other point of the Hilbert space have a limited practical usefulness, although, in this case as shown in Ref. 3, in principle, it is possible to derive a scheme to control the evolution of the state vector to a desired final state.

Until now, quantum control was mainly applied to electronic transitions between discrete energy levels, for example, in molecular dynamics,⁴⁻⁹ or transitions between quantum wells.¹⁰⁻¹² Recently, the problem was extended to polaritons,¹⁸ phonons,¹⁹ and to electronic transitions between energy bands.¹⁴⁻¹⁶ Due to mathematical difficulties most of the quantum-control problems were treated numerically. The control of charge carrier transitions between the bands was solved using either the nonlinear programming method^{14,15} or the genetic algorithm.¹⁶ Some analytically tractable problems, for example, the optimal control of electron spin flipping by time-varying magnetic fields in a two-level system, can be found in the book by Butkovskiy and Samoilenko.²

In this paper, a simple two-band model based on the Luttinger-Kohn Hamiltonian is solved analytically with the aim to obtain a deeper understanding of the properties of optimal control in the case of extended energy bands. The model is rather general and is not limited to free holes. The

results can be applied to electronic transitions as well. The charge carriers that participate in the interband transition can be provided by donors, acceptors, or injection currents. This paper considers only noninteracting carriers; therefore, the injection or doping levels should be low, for example, the carrier concentration should be lower than 10^{15} cm^{-3} at room temperature. The paper is limited to single-carrier optimal transitions. The case of distribution of carriers is more difficult and not considered here. Some preliminary results obtained with numerical methods are presented in Ref. 17. In Sec. II, starting from the Luttinger-Kohn Hamiltonian a two-band model is reduced to a simple time-dependent equation that describes population transfer dynamics between two energy bands. In Sec. III, the Euler differential equation for optimal interband transitions is obtained, and in Sec. IV a numerical solution of the Euler equation is presented as an illustration.

II. TWO-BAND EQUATION

An effective-mass Hamiltonian that describes valence band of the elementary semiconductors will be used as a starting point:^{20,21}

$$\hat{H}_0 = \frac{M+N}{2} \mathbf{k}^2 - \frac{N}{2} (\mathbf{k}\hat{\mathbf{I}})^2. \quad (1)$$

In Hamiltonian (1), M and N are the valence-band parameters and, $\mathbf{k} = (k_x, k_y, k_z)$ is the hole wave vector, the components of which are measured with respect to Cartesian axes. The Hamiltonian is constructed in terms of the spin operator $\hat{\mathbf{I}} = (\hat{I}_x, \hat{I}_y, \hat{I}_z)$, where

$$\hat{I}_x = \begin{vmatrix} 0 & 0 & 0 \\ 0 & 0 & -i \\ 0 & i & 0 \end{vmatrix}, \quad \hat{I}_y = \begin{vmatrix} 0 & 0 & i \\ 0 & 0 & 0 \\ -i & 0 & 0 \end{vmatrix}, \quad \hat{I}_z = \begin{vmatrix} 0 & -i & 0 \\ i & 0 & 0 \\ 0 & 0 & 0 \end{vmatrix}, \quad (2)$$

and $i = \sqrt{-1}$. The spin matrices (2) satisfy standard commutation relations and $\hat{I}_x^2 + \hat{I}_y^2 + \hat{I}_z^2 = 2$. Atomic units ($e = \hbar = m = 1$) are used in this paper. The quadratic Hamiltonian (1) represents energy surfaces with maximal (triple) degeneracy at the center of the Brillouin zone. The eigenvalues of Eq. (1)

describe two parabolic and spherical energy bands: the doubly degenerate heavy-mass (h) band and single nondegenerate light-mass (l) band with the following dispersion laws:

$$\varepsilon_h = M\mathbf{k}^2/2, \quad (3)$$

$$\varepsilon_l = (M+N)\mathbf{k}^2/2. \quad (4)$$

The parameters M and N can be expressed through heavy- and light-hole masses. It should be noted that the considered problem is not limited to valence band only. It applies to any bands described by spherical and parabolic dispersion laws. If needed band degeneracy at the point $\mathbf{k}=\mathbf{0}$ can be lifted. In the following the more general case with the degeneracy included will be analyzed. The electric field \mathbf{F} of electromagnetic radiation couples the bands. If the field is switched on, say, at moment $t=0$, then at later moments the population or the probability to detect the hole in a particular band will depend on time. In the presence of the electric field the corresponding Schrödinger equation for three-component wave function ψ will be written in the following way:²¹

$$i\frac{\partial\psi}{\partial t} = \left(\hat{H}_0 + \frac{\mathbf{F}(t)}{i} \frac{\partial}{\partial\mathbf{k}} \right) \psi. \quad (5)$$

In the case of energy bands the time dependence of the wave vector \mathbf{k} is described by the equation²²

$$d\mathbf{k}/dt = \mathbf{F}(t). \quad (6)$$

In our case Eq. (6) is redundant since it is a characteristic equation of the solved Schrödinger system (5). Equation (6) will be used later to obtain a set of ordinary differential equations. Due to the high symmetry of the problem, the solution of the system (5) is not unique. In Ref. 23 it was shown that for spherical bands the interband transitions between degenerate and nondegenerate bands could be partially decoupled. The corresponding unitary transformation operator \hat{T} that decouples the bands was constructed in Ref. 23. Recently, a more general transformation operator was found for the full valence-band Hamiltonian, where the split-off band and nonparabolicity of constant energy surfaces was included too.²⁴ For definiteness, in the following it will be assumed that optical electric field is linearly polarized and parallel to the k_z direction, i.e., $\mathbf{F}=(0,0,F_z)$. Then, as shown in Ref. 23 there exists an orthogonal transformation matrix $\hat{T}(\alpha)$, where α is an arbitrary parameter, that diagonalizes the Hamiltonian (1): $\hat{H}_d = \hat{T}^{-1}(\alpha)\hat{H}_0\hat{T}(\alpha)$. The diagonal elements in \hat{H}_d represent the dispersion equations (3) and (4). The matrix $\hat{T}(\alpha)$ allows us to transform Eq. (5) into an energy representation. In this representation the Schrödinger system (5) assumes the following form:

$$i\frac{\partial}{\partial t} \begin{pmatrix} \varphi_1 \\ \varphi_2 \\ \varphi_3 \end{pmatrix} = \left\{ \begin{pmatrix} \varepsilon_l & 0 & 0 \\ 0 & \varepsilon_h & 0 \\ 0 & 0 & \varepsilon_h \end{pmatrix} + \frac{F_z}{i} \begin{pmatrix} \partial/\partial k_z & -\beta \sin \alpha & -\beta \cos \alpha \\ \beta \sin \alpha & \partial/\partial k_z & 0 \\ \beta \cos \alpha & 0 & \partial/\partial k_z \end{pmatrix} \right\} \begin{pmatrix} \varphi_1 \\ \varphi_2 \\ \varphi_3 \end{pmatrix}. \quad (7)$$

The three-component column function φ is related to ψ via transformation $\varphi = \hat{T}^{-1}(\alpha)\psi$. The component $|\varphi_i|^2$ gives the population of the i th band. An explicit matrix for the operator $\hat{T}(\alpha)$ can be found in Ref. 23. The second matrix in the transformed Schrödinger equation (7) represents the interband coupling matrix. The parameter $\beta = k_\perp / (k_\perp^2 + k_z^2)$, where $k_\perp = \sqrt{k_x^2 + k_y^2}$ is the wave vector perpendicular to electric field, plays the role of a coupling coefficient, which, due to Eq. (6), depends on time. In the coupling matrix the parameter α is an arbitrary constant that comes out of the general transformation operator $\hat{T}(\alpha)$. Equation (7) shows that the light-mass band may be coupled either to $h1$ or to $h2$ of the two degenerate heavy-mass bands by choosing either $\alpha=0$ or $\alpha=\pi/2$. In the general case, the l band may be coupled to both heavy-mass bands simultaneously if an intermediate value of α is chosen. It should be noted that the parameter α is absent in the initial formulation of the problem in Eq. (5). The free parameter, or more precisely the function $\tan \alpha$, in fact, represents the ratio of the coupling of the l band to $h1$ and $h2$ bands. As shown in Ref. 25, the hidden symmetry of the problem is revealed as chaotic oscillations between doubly degenerate $h1$ and $h2$ bands, if one tries to solve the system (5) numerically and uses a numerical unitary transformation to obtain the evolution of hole populations in the bands in the presence of the optical field. Thus, before attempting to find a concrete solution of the transformed equation (7) one must at first assign a numerical value to α . In the following we shall assume that $\alpha = \pi/2$, i.e., only electronic transitions between bands characterized by wave functions $\varphi_1 \equiv \varphi_h$ and $\varphi_2 \equiv \varphi_l$ will be considered.

It can be shown that solution of the wave vector equation (6) is the characteristic equation of partial differential equation (5). Using this property and the relation between total and partial derivatives, $d\varphi_i/dt = \partial\varphi_i/\partial t + F_z\partial\varphi_i/\partial k_z$, one can reduce Eq. (5) from partial derivatives to total derivatives. Remembering that $\alpha = \pi/2$, one gets the following two coupled equations from Eq. (7):

$$i\frac{d\varphi_1}{dt} = \frac{M+N}{2}\mathbf{k}^2\varphi_1 + iF_z\beta\varphi_2, \quad (8)$$

$$i\frac{d\varphi_2}{dt} = \frac{M}{2}\mathbf{k}^2\varphi_2 - iF_z\beta\varphi_1. \quad (9)$$

The time-dependent system (8) and (9) is rather general. If needed, the degeneracy at the point $\mathbf{k}=\mathbf{0}$ can be lifted by adding a constant term to the first right-hand-side term in

either Eq. (8) or (9). The coupling between bands depends on \mathbf{k} . It is small at large wave vectors, which is physically acceptable. In the following, we shall show that further simplification of the resulting equations (8) and (9) is possible. Since we are interested in optimal control of measurable quantities rather than the control of evolution of the state vector φ in the Hilbert space, it appears possible to simplify the problem in this case to a single time-dependent equation. If instead of φ_1 and φ_2 , new functions R and ϕ are introduced with the help of relations

$$\varphi_1 = R \cos \phi, \quad \varphi_2 = R \sin \phi, \quad (10)$$

then, remembering that $\beta = k_{\perp}/k^2$, one gets the following coupled equations for R and ϕ from Eqs. (8)–(10):

$$i \frac{dR}{dt} = \frac{\mathbf{k}^2}{2} (M + N \cos^2 \phi) R, \quad (11)$$

$$\frac{d\phi}{dt} = \frac{i\mathbf{k}^2}{4} N \sin 2\phi - F_z \beta. \quad (12)$$

One should note that in Eq. (12) only the energy difference $N\mathbf{k}^2/2 = \varepsilon_l - \varepsilon_h$ between the bands at the point \mathbf{k} rather than the absolute band energies is of importance. If one is interested in carrier population dynamics in respective bands only, then one can show²⁶ that it is not needed to know the solution of function R . Thus, the problem of band population dynamics reduces to a single equation (12) and the probability to find the carrier in the heavy- or light-mass band, P_h or P_l , at the moment t reduces to calculation of real and imaginary parts of ϕ only. Since $P_l = |\varphi_1(t)|^2$ and $P_h = |\varphi_2(t)|^2$, then using Eqs. (10)–(12) it can be shown that

$$P_l = (1 - \cos 2\phi_r / \cosh 2\phi_i) / 2, \quad (13)$$

$$P_h = (1 + \cos 2\phi_r / \cosh 2\phi_i) / 2, \quad (14)$$

where ϕ_r and ϕ_i are the real and imaginary parts of ϕ . Equations (13) and (14) at the same time yield the initial condition for ϕ in Eq. (12). If, for example, at $t=0$ the carrier was in the heavy-mass band with probability $P_h = 1$, then as follows from Eqs. (13) and (14) the initial conditions $\phi_r(0) = 0$ and $\phi_i(0) = 0$ should be satisfied at the moment $t=0$. In Secs. III and IV we shall be interested in optimum population dynamics; therefore only Eq. (12) will be used in the optimal control model.

Figure 1 shows the probability P_l to find the carrier in l band as a function of time calculated with Eqs. (6) and (12) under various types of excitation $F_z(t)$, assuming that $N = 12$ and that at the initial moment the probabilities are $P_l = 0$ and $P_h = 1$. The stepped electric field (curve 1) that was switched on at $t=0$ yields only transient interband excitation of small amplitude, $P_l(t) < 0.045$. The harmonically varying field, the frequency ω of which is tuned to resonance $\omega = \varepsilon_l(\mathbf{k}_0) - \varepsilon_h(\mathbf{k}_0) = 0.0012$ a.u., where $\mathbf{k}_0 = (0.01, \sqrt{0.01}, \sqrt{0.01})$ a.u. is the initial wave vector, yields periodic Rabi oscillations of band population [curve 2 in panel (b)]. Curve 3 in panel a shows the Gaussian-shaped π

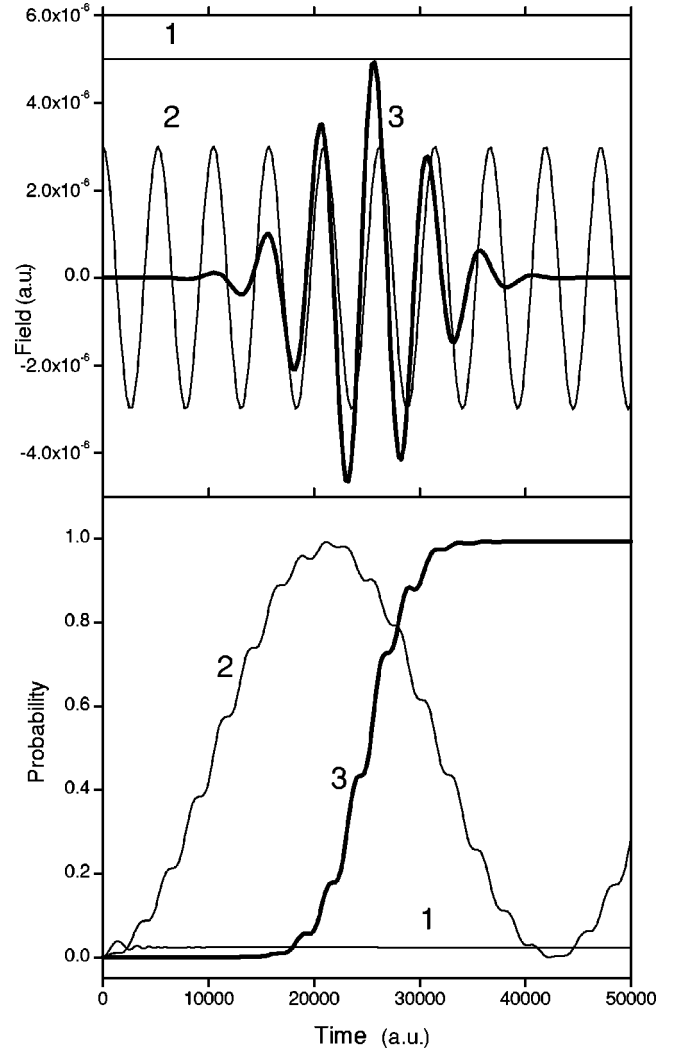


FIG. 1. (a) Three shapes of the electric field switched on at the moment $t=0$ and (b) time dependence of corresponding probabilities to detect the hole in l -band as calculated with Eqs. (6) and (12). 1, stepped electric field; 2, resonant harmonic field; 3, Gaussian π pulse.

pulse, and the respective curve in panel (b) shows the evolution of the probability P_l from zero to unity.

Thus, the main result of this section is that the two-band population dynamics can be reduced to a single dynamical transition equation (12), which depends on the energy difference $\Delta\varepsilon = \varepsilon_l(\mathbf{k}) - \varepsilon_h(\mathbf{k}) = N\mathbf{k}^2/2$ between the bands rather than on the absolute energies of the bands. The main equation (12) bears some resemblance to the classical nonlinear oscillator equation, although Eq. (12) is complex and should be solved simultaneously with the wave vector equation (6).

III. VARIATIONAL CALCULATION OF OPTIMAL FIELD

In this section the Euler equation for optimal electronic transitions between two energy bands is deduced. The variational problem becomes analytically treatable if instead of time t a new variable $z = k_z(t)/k_{\perp}$ is introduced, and the complex trigonometric function in Eq. (12) is eliminated in

favor of the new variable $y = \tan \phi$. Then, the following differential equations for real and imaginary parts of y can be obtained from Eq. (12):

$$\frac{dy_r}{dz} = -\frac{\varepsilon_{\perp}}{f}(1+z^2)y_i - \frac{1+y_r^2-y_i^2}{1+z^2}, \quad (15)$$

$$\frac{dy_i}{dz} = \frac{\varepsilon_{\perp}}{f}(1+z^2)y_r - \frac{2y_i y_r}{1+z^2}, \quad (16)$$

where $\varepsilon_{\perp} = k_{\perp}^2 N/2$ and $f(t) = F_z(t)/k_{\perp}$. The probabilities (13) and (14) reduce to

$$P_l = yy^*/(1+yy^*), \quad P_h = 1/(1+yy^*). \quad (17)$$

Since the transverse wave vector is the constant of motion, the energy ε_{\perp} is the constant of motion too. Equations (15)–(17) and the normalized wave vector equation for component k_z

$$dz/dt = f \quad (18)$$

make up a closed system in the analysis of the optimized interband transitions.

In the following the Euler equation for $y_i(z)$ is deduced. For this purpose, we shall solve the terminal optimization problem with the quadratic optimization criterion.² Let field F_z act the carrier that participates in the interband transition during time interval $\Delta t = (0 - t_f)$, where t_f is the final or terminal time. The quadratic functional

$$J[y_i(z)] = \int_0^{t_f} F_z^2 dt \quad (19)$$

will be used to construct the Euler equation. The functional (19) requires the total energy of the pulse to be minimal. It should be noticed that, in fact, the energy of the pulse will be minimal at any value of t_f , in other words, at any beforehand assumed final time. In the functional (19), the argument $y_i(z)$ indicates that we are interested in the optimization of $y_i(z)$ trajectory in the complex y plane. The trajectory of $y_r(z)$ remains undefined. Of course, instead of the imaginary part one can use real part $y_r(z)$, or even modulus $|y|$ in the optimization of interband transitions. Using the normalized characteristic equation (18), the quadratic functional can be transformed to a linear one:

$$J[y_i(z)] = k_{\perp}^2 \int_0^{t_f} f dz. \quad (20)$$

Then, after expressing the field from Eq. (16), the functional becomes

$$J[y_i(z)] = \int_0^{t_f} \frac{\varepsilon_{\perp} k_{\perp}^2 (1+z^2) y_r}{y_i' + 2y_i y_r / (1+z^2)} dz, \quad (21)$$

where $y_i' \equiv dy_i/dz$. This functional yields the following second-order Euler differential equation with respect to $y_i(z)$,

$$a_2 y_i'' + a_1 y_i' + b_1 (y_i')^2 + a_0 = 0, \quad (22)$$

where coefficients are z -dependent functions:

$$a_0 = 2y_i y_r (1 + 3y_i^2 - y_r^2 + 6y_r z), \quad (23)$$

$$a_1 = (1+z^2)(-1 - y_i^2 + 2z y_r - 7y_r^2), \quad (24)$$

$$a_2 = -2(1+z^2)^2 y_r, \quad (25)$$

$$b_1 = -(1+z^2)^2 y_i / y_r. \quad (26)$$

If f is expressed from Eq. (16) and then inserted into Eq. (15), then the resulting equation and Euler equation (22) form a closed system for finding optimal electric fields.

The obtained Euler equation (22) is highly nonlinear and analytically untractable. Since the interband coupling coefficient $\beta = k_{\perp} / [k_z^2(t) + k_{\perp}^2]$ is a time-varying function (due to parallel to the F_z wave vector), to simplify the problem further it is tempting to assume that β is constant and then to try to solve the variational problem with constant interband coupling from the beginning, hoping to obtain a simpler Euler equation. I have deduced such equation for a constant coupling too. The resulting Euler equation in this case was found to have the same structure as Eq. (22) and the nonlinearity of the equation was of the same order. Furthermore, I have found that, independent of which wave functions y_i , y_r , ϕ_r , etc. was used to obtain the Euler equation, in all cases the same structure of the nonlinear Euler equation has resulted.

Before ending this section, a short discussion on boundary conditions will be presented. The solution of the Euler equation must satisfy terminal boundary conditions at $t=0$ and $t=t_f$, i.e., one must assume the boundary values $y_i(z_0)$ and $y_i(z_f)$ in Eq. (22). As explained after Eq. (14), the initial conditions and band populations are related. For definiteness, if we assume that at $t=0$ the hole was in heavy-mass band with the probability $P_h(0) = 1$, then one must satisfy $y(z_0) = 0$, which means that at the initial moment both the real and imaginary parts must be equal zero: $y_i(z_0) = y_r(z_0) = 0$. These initial conditions and the condition $y_i(z_f)$ are sufficient to solve Eqs. (15) and (22) with respect to $y_i(z)$ and $y_r(z)$. However, the function $y(z)$, in general, is a complex quantity and, therefore, the real part $y_r(z_f)$ remains arbitrary at the terminal times t_f . From this we conclude that our optimal control problem is not unique. This is also reflected in the fact that, for example, one may also work with the Euler equation for the modulus of y . Then, the final phase of y will be an arbitrary terminal function. In the following it will be assumed that before application of the field, at $t=0$, the carrier with certainty was in the h band and the final transition probability at t_f satisfies $P_l(z_f) \approx 1$. Then the function $y_r(z_f)$ will remain undefined. Figure 2 shows one of many possible optimal trajectories in the complex y plane under the described boundary conditions. The dashed lines in Fig. 2 show the equations $y_i = \pm d$. Under assumed boundary conditions, if one wants to transfer the hole from the h to l band, the trajectory should begin at the point $y=0$ and end up in the upper or lower half of the plane, where $|y_i(z_f)| \gg |d| \gg 1$. This boundary condition requires an apparatus that

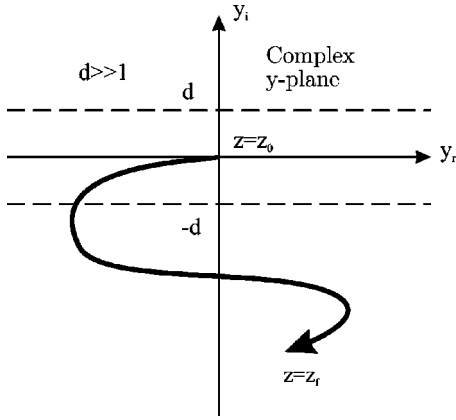


FIG. 2. A typical trajectory of transient wave function in a complex y plane for optimal control, when initially the hole was in heavy-mass band.

measures the probability $P_l(t_f) = y_i^2(t_f)/[1 + y_i^2(t_f)] \approx 1$ of the hole being in the l band at t_f and which, at the same time, does not perturb $y_r(t_f)$, i.e., the quantity y_r , in principle, should remain an unobservable during the measuring process. As mentioned, it is possible to construct the Euler equation for modulus $|y|$ too. Then the measuring apparatus should measure the probability $P_l = |y|^2/(1 + |y|^2)$ and leave the phase of the wave function unperturbed.

In this section it was demonstrated explicitly that there exist multiple solutions to a well-posed quantum-mechanical interband optimal control problem. In the next section an example of the interband control is presented.

IV. EXAMPLE

It is convenient to rewrite the obtained equations for optimal transitions as a system of three first-order differential equations. Then, after introduction of new variables $u_1 = y_i$, $u_2 = y_r$, $u_3 = dy_i/dz$, one has

$$u'_1 = u_3, \quad (27)$$

$$u'_2 = - \left(u_3 + \frac{2u_1u_2}{1+z^2} \right) \frac{u_1}{u_2} - \frac{1+u_2^2-u_1^2}{1+z^2}, \quad (28)$$

$$u'_3 = -(a_1/a_2)u_3 - (b_1/a_2)u_3^2 + a_0/a_2. \quad (29)$$

The new functions satisfy the following boundary conditions: $u_1(z_0) = u_2(z_0) = 0$, $u_1(z_f) \gg 1$, where z_0 and z_f are the initial and final normalized wave vectors, respectively. It should be noted that the system (27)–(29) is independent of band parameters N and M . Numerical solution of this system by standard differential equation solvers is difficult because Eqs. (28) and (29) are singular: their right-hand sides are infinite at some points on the z axis where $y_r(z) = 0$. Near these singular points Eqs. (28) and (29) may be simplified. Leaving the leading terms on the right-hand sides of Eqs. (28) and (29), one obtains

$$u'_2 \approx -u_1u_3/u_2, \quad (30)$$

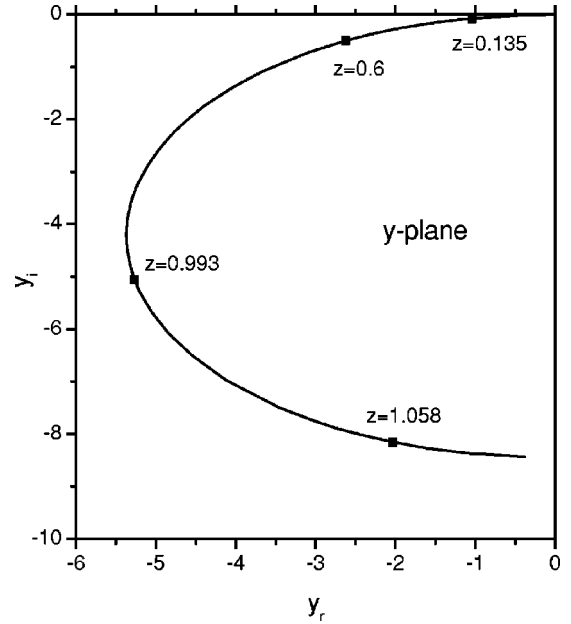


FIG. 3. Optimal trajectory on the complex y plane found from the simultaneous solution of Eq. (15) and the Euler equation (22). The terminal values of z are $z_0 = -0.8$ and $z_f = 1.067$.

$$u'_3 \approx \frac{u_3}{2(1+z^2)u_2} - \frac{u_1}{2} \left(\frac{u_3}{u_2} \right)^2. \quad (31)$$

It is seen that the singularities come from the term $u_3/u_2 \equiv y'_i/y_r$. The primary source of singularities can be traced from Eq. (16), from which follows that

$$y'_i/y_r \approx (\varepsilon_{\perp}/f)(1+z^2). \quad (32)$$

It is clear that the singularities appear at the points where the electric field goes through zero. In the vicinity of these points the evolution of the solution should be analyzed in terms of the primary parameter t , for example, with the help of Eqs. (15) and (16), rather than in terms of the normalized wave vector z . We shall limit the analysis to monopolar field pulses and assume that at the moment $t=0$ the field is finite and has very small value. This will allow us to find the solution numerically between two singular points and avoid the problem of regularization of the solution. Then, from primary equations (15) and (16) follows that at $t=0$ instead of boundary conditions at z_0 and z_f one can approximately assume the following zero and nonzero conditions at the boundary point z_0 only: $u_1(z_0) = 0$, $u_2(z_0) \neq 0$, and $u_3(z_0) \neq 0$. This means that for monopolar pulses the problem can be reduced to the initial value problem, which is similar to the shooting method in the two-point boundary value problems.²⁷

Figure 3 shows the trajectory in the y plane calculated numerically with Eqs. (27)–(29) and (32) using the following input parameters: $\varepsilon_{\perp} = 10^{-4}$ a.u., $f = 4 \times 10^{-6}$ a.u., $z_0 = -0.8$, $z_f = 1.067$, $u_1(z_0) = 0$, and $u_2(z_0) = 10^{-3}$. Figure 4 shows the probability P_l and field f as a function of time (the points in Fig. 4 are plotted at equal Δz intervals: $\Delta z = z_f/100$). The field was deduced from Eq. (16),

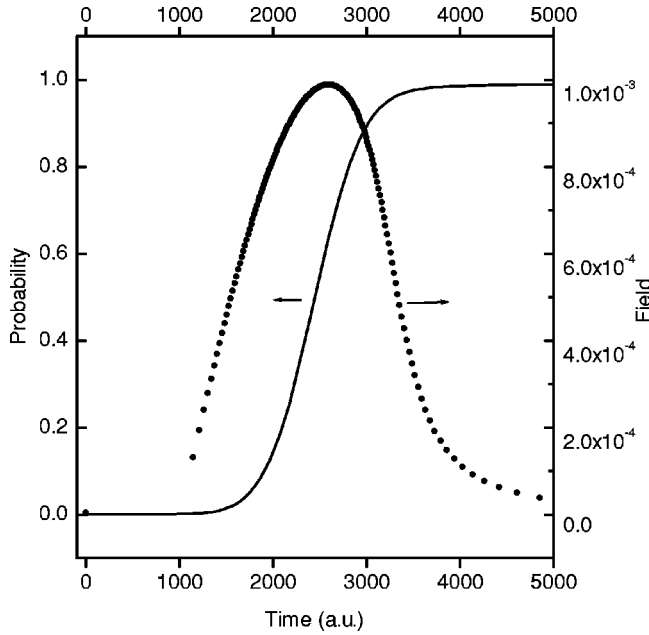


FIG. 4. Time dependence of optimal control field f (dots) and excitation probability P_l (line) calculated from Fig. 3.

$$f(z) = \frac{\varepsilon_{\perp}(1+z^2)u_2}{u_3 + 2u_1u_2/(1+z^2)}. \quad (33)$$

The coordinate z was transformed to time after numerical integration of Eq. (18). The following features should be noted in Fig. 4. The maximum amplitude of the pulse is $f_{\max} = F_{\max}/k_{\perp} \approx 10^{-3}$ a.u., or $F_{\max} = 2.1 \times 10^4$ V/cm if k_{\perp} is calculated from ε_{\perp} and $N=12$ is used. The transition probability changes significantly only in the middle portion of the electric pulse. At the beginning and end of the pulse

the field changes slowly; as a result oscillations in the transition probability are absent and the probability is a monotonic function of time (compare the oscillating character of the probability in Fig. 1, where a stepped electric field is applied). The width of the optimal pulse at half-amplitude is very short, about 2000 a.u. ≈ 48 fs. The obtained character of interband transitions should also be compared with that in Fig. 1, where a Gaussian π pulse was used to transfer the hole from the h to l band. The width of the optimal pulse is comparable to the one calculated from the energy-time uncertainty relation $\Delta t \Delta \varepsilon = 1$, where $\Delta \varepsilon$ is the energy gained from the field by the carrier: $\Delta \varepsilon = \varepsilon_l(t_f) - \varepsilon_h(0) = (2M/N)\varepsilon_{\perp}(z_f^2 - z_0^2) + 2\varepsilon_{\perp}(z_f^2 + 1)$. If one assumes that $M=0$, i.e., that the h band is flat, then the second term gives $\Delta \varepsilon = 4 \times 10^{-4}$ a.u. or $\Delta t \approx 2500$ a.u., which is comparable to pulse half-width. For practical applications this means that optimal interband switching is faster in those materials where energy separation between conduction or valence bands is larger.

In summary, a simple model that describes interband transition dynamics between two parabolic and spherical energy bands in the presence of optical field was constructed. The model consists of a single first-order differential equation for the transition wave function rather than of two equations for coupled band wave functions. With this model it appeared possible to solve the variational problem of interband control analytically and to demonstrate explicitly the multiplicity of solutions of a quantum-mechanical optimal control problem. In case of monopolar pulses, the solution of the Euler equation yields a smooth transition probability from one band to another band during a time interval, the length of which is of the order of inverse absorbed total energy by the carrier from the field. Such ultrashort and optimized π pulses have a potential application in quantum control, femtosecond spectroscopy, and quantum computers.

*Email address: dargys@uj.pfi.lt

¹A. G. Butkovskiy and Y. I. Samoilenko, Dokl. Akad. Nauk SSSR **250**, 51 (1980).

²A. G. Butkovskiy and Y. I. Samoilenko, *Control of Quantum Mechanical Processes* (Nauka, Moscow, 1984) (in Russian).

³G. M. Huang, T. J. Tarn, and J. W. Clark, J. Math. Phys. **24**, 2608 (1983).

⁴A. P. Peirce, M. A. Dahleh, and H. Rabitz, Phys. Rev. A **37**, 4950 (1988).

⁵M. Dahleh, A. P. Peirce, and H. Rabitz, Phys. Rev. A **42**, 1065 (1990).

⁶S. H. Tersigni, P. Gaspard, and S. A. Rice, J. Chem. Phys. **93**, 1670 (1990).

⁷S. Chelkowski, A. D. Bandrauk, and P. B. Corkum, Phys. Rev. Lett. **65**, 2355 (1990).

⁸J. F. Krause, R. M. Whitnell, K. R. Wilson, Y. J. Yan, and Sh. Mukamel, J. Chem. Phys. **99**, 6562 (1993).

⁹B. Kohler, V. V. Yakovlev, J. Che, J. L. Krause, M. Messina, K. R. Wilson, N. Schwentner, R. M. Whitnell, and Y. Yan, Phys. Rev. Lett. **74**, 3360 (1995).

¹⁰A. V. Kuznetsov, G. D. Sanders, and C. J. Stanton, Phys. Rev. B **52**, 12 045 (1995).

¹¹J. L. Krause, D. H. Reitze, G. D. Sanders, A. V. Kuznetsov, and C. J. Stanton, Phys. Rev. B **57**, 9024 (1998).

¹²M. S. C. Luo, S. L. Chuang, P. C. M. Planken, I. Brener, and M. C. Nuss, Phys. Rev. B **48**, 11 043 (1993).

¹³M. Demiralp and H. Rabitz, Phys. Rev. A **47**, 809 (1993).

¹⁴A. Dargys, Phys. Status Solidi B **219**, 401 (2000).

¹⁵A. Dargys, Proc. SPIE **4318**, 157 (2001).

¹⁶A. Dargys, Topol. Methods Nonlinear Anal.: Modeling and Control **6**, 27 (2001).

¹⁷A. Dargys, in *Proceedings of the 11th International Symposium on Ultrafast Phenomena in Semiconductors, Vilnius, August, 2001*, Mat. Sci. Forum (accepted).

¹⁸P. Renucci, X. Marie, T. Amand, M. Paillard, and J. Barrau, Superlattices Microstruct. **26**, 61 (1999).

¹⁹V. M. Axt, M. Herbst, and T. Kuhn, Superlattices Microstruct. **26**, 117 (1999).

²⁰J. M. Luttinger and W. Kohn, Phys. Rev. **97**, 869 (1955).

²¹G. L. Bir and G. E. Pikus, *Symmetry and Strain-Induced Effects in Semiconductors* (Wiley, New York, 1974), Chap. IV.

²²C. Kittel, *Quantum Theory of Solids* (Wiley, New York, 1963), Chap. IX.

²³A. Dargys and A. F. Rudolph, Phys. Status Solidi B **140**, 535 (1987).

²⁴A. Dargys, Phys. Rev. B **59**, 4888 (1999).

²⁵A. Dargys, Lith. J. Phys. **40**, 431 (2000).

²⁶In calculating P_h and P_l apart from ϕ we need the product RR^* , where R^* is the complex conjugate of R . However, the integral that appears in the exponent of RR^* after integration of Eq. (11) can be expressed in terms of ϕ_i if real and imaginary parts in

Eq. (12) are separated and then used to change the integration variable in RR^* to ϕ_i .

²⁷W. H. Press, S. A. Teukolsky, W. T. Vetterling, and B. P. Flannery, *Numerical Recipes in Fortran* (Cambridge, University Press, 1992), Chap. 17.